SLAC–PUB–10044
CEA-DAPNIA-SPHN-94-52
October 1994

Last Experimental Results Obtained at SLAC on the Nucleon Spin Structure*

Y. Terrien
DAPNIA/SPhN, CE-Saclay, 91191 Gif/Yvette Cedex, France

On behalf of the E142-E143 Collaborations
Stanford Linear Accelerator Center, Stanford, California, 94309

Presented at the 12th International Seminar on High Energy Physics Problems: Relativistic Nuclear Physics and Quantum Chromodynamics (ISHEPP 94)

Dubna, Russia

September 13-17, 1994

* Work supported in part by Department of Energy contract DE–AC03–76SF00515.

LAST EXPERIMENTAL RESULTS OBTAINED AT SLAC ON THE NUCLEON SPIN STRUCTURE

Yves TERRIEN
DAPNIA/SPhN, CE-Saclay,
91191 Gif/Yvette Cedex, France

On behalf of the E142-E143 collaborations
SLAC, Stanford Univ., USA

Abstract: Recent precise measurements of the spin structure function g_1 for proton and for deuteron using deep inelastic scattering of polarized electrons from polarized ammonia targets are presented. The integrals $\Gamma_1 = \int_0^1 g_1(x)dx$ evaluated at the average experimental Q=3 $(\mathrm{GeV/c})^2$ are in agreement with previous results and well below the Ellis-Jaffe sumrule prediction, while the Björken sumrule prediction on $\Gamma_1^p - \Gamma_1^n$ is satisfied. The analysis of the results in term of Quark Parton Model implies that the quark carry about a third of the nucleon helicity.

Introduction

In the beginning of the eighties, a "spin crisis" was opened by the results of the SLAC[1,2] and EMC[3] experiments of Deep Inelastic Scattering (DIS) of a polarized electron beam from a polarized proton target. Indeed, the experimental results were interpreted as being in contradiction with the simple Quark Parton Model (QPM) in which the spin of the nucleon results from the combination of the spins of the 3 u or d valence quarks coupled together in a S-state of relative momenta. Also, the so-called Ellis-Jaffe Sum Rule[4] (EJSR) on the structure function $g_1^p(x)$ of the proton appeared to be violated, which could mean that the strange s quark contributes to the nucleon spin. Then, a lot of papers issued, proposing many possible explanations to these results. Rapidly, it appeared that comparable experiments on neutron or, alternatively, deuteron targets were eagerly wanted to see if the deviations from QPM and EJSR were similar, and since the knowledge of both $g_1^p(x)$ and $g_1^n(x)$ permits to test the Björken Sum Rule (BSR)[5], theoretically much better founded than the EJSR. So, in the last years, an extensive program of polarized lepton DIS from polarized nucleon targets has been undertaken and is still currently in progress, both at CERN (muon secondary beams) or at SLAC (electron beam).

The present paper recalls the results obtained by the E142 collaboration to measure $g_1^n(x)$ (polarized ^{3}He target) and presents the results obtained by the E143 collaboration to measure $g_1^p(x)$ and $g_1^d(x)$ (polarized NH_3 and ND_3 targets). Both experiments were done at SLAC. After a brief recall of the physical background in Sect. 1, the experimental apparatus and procedure will be described in Sect. 2 and the results and their analysis will be developed in Sect. 3 before conclusion.

1 – The physical background :

The nucleon spin results from the quarks spins combination, from their relative angular momenta inside the nucleon and from a possible gluon contribution. In lepton induced scattering, the lepton couples to the individual quarks via an exchange of a virtual photon, which permits to obtain information (the so-called structure functions) on the quarks distribution inside the nucleon. In case of an experiment using polarized beam and target, the contribution of the quarks to the nucleon spin can be estimated.

In inclusive DIS of longitudinally polarized lepton from longitudinally polarized nucleon, the difference between the cross-sections for parallel and antiparallel spins of the beam and the target is given by

$$\frac{d^3\sigma}{d\Omega dE'}(\downarrow\uparrow\ -\ \uparrow\uparrow) = \frac{4\alpha^2 E'^2}{EQ^2}\{(E + E'\cos\theta)M\mathrm{G}_1(\nu, Q^2) - Q^2\mathrm{G}_2(\nu, Q^2)\}$$

where $G_1(\nu,Q^2)$ and $G_2(\nu,Q^2)$ are functions depending on the transferred energy ν and momentum Q^2, E and E' are the incident and scattered energies respectively and Θ is the scattering angle. If the spins of the beam and of the target are perpendicular, a similar relation holds:

$$\frac{d^3\sigma}{d\Omega dE'}(\downarrow\leftarrow\ -\ \uparrow\leftarrow) = \frac{4\alpha^2 E'^2}{EQ^2}E'\sin\theta\{M\mathrm{G}_1(\nu, Q^2)+2E\mathrm{G}_2(\nu, Q^2)\}$$

Related to the fact that nucleons are made of partons, in the limit where $Q^2 \rightarrow \infty$ and $\nu \rightarrow \infty$, one has

$$M^2 \nu G_1(\nu, Q^2) \rightarrow g_1(x) \text{ and } M\nu^2 G_2(\nu, Q^2) \rightarrow g_2(x)$$

where $x = Q^2/2M\nu$ and M is the nucleon mass. This scaling variable is the so-called Björken variable, $g_1(x)$ and $g_2(x)$ are the spin structure functions of the nucleon.

First derived by Björken[5] as a consequence of basic current algebra, then shown to be a direct consequence of QCD, the Björken Sum Rule predicts that:

$$\Gamma_1^p - \Gamma_1^n = \int_0^1 \left(g_1^p(x) - g_1^n(x)\right) dx = \frac{1}{6}\frac{g_A}{g_V}$$

where g_A and g_V are the axial and vector coupling constants of the neutron decay. This BSR is very fundamental and is expected to be satisfied.

Then, Ellis and Jaffe[4] showed that, with the extra assumptions that the SU(3) symmetry is valid and that the strange sea is unpolarized, the integral of $g_1(x)$ must satisfy, separately for the proton and for the neutron, the so-called Ellis-Jaffe Sum Rules:

$$\Gamma_1^p = \int_0^1 g_1^p(x) dx = \frac{1}{12}\frac{g_A}{g_V}\left[1 + \frac{5}{3}\frac{3F/D - 1}{F/D + 1}\right]$$

$$\Gamma_1^n = \int_0^1 g_1^n(x) dx = \frac{1}{12}\frac{g_A}{g_V}\left[-1 + \frac{5}{3}\frac{3F/D - 1}{F/D + 1}\right]$$

where F/D is the ratio of the nucleon axial charges in terms of SU(3) matrix parametrization. The above BSR and EJSR equations have to be corrected at all orders of the leading constant α_s of QCD. This is a key point since all experiments done at SLAC or at CERN are done at moderate Q^2 values, which means that these perturbative QCD corrections are important (see Sect.3).

At last, one usually defines $\Delta u = \int_0^1 \left[u^+(x) - u^-(x)\right] dx$ where u^+ and u^- are the probabilities to find the flavour-u quark with the fraction x of the momentum of the nucleon and with an helicity the same (+) or opposite (-) to that of the nucleon, and defining Δd and Δs the same way. The first moments $\Gamma_1^{p,n}$ are related to the SU(3) matrix elements a_0, a_3 and a_8 through the equation:

$$\Gamma_1^{p,n} = \pm\frac{a_3}{12}(1 - C_{NS}) + \frac{a_8}{36}(1 - C_{NS}) + \frac{a_0}{9}(1 - C_S)$$

where C_{NS} and C_S are the perturbative non-singlet and singlet QCD corrections (vanishing at infinite Q^2). Then, the relations between the Δq's, the SU(3) matrix elements and the F and D coefficients measured in neutron and hyperons weak decays are given by:

$$\Delta u - \Delta d = a_3 = F + D$$
$$\Delta u + \Delta d - 2\Delta s = a_8 = 3F - D$$
$$\Delta u + \Delta d + \Delta s = a_0$$

So, F and D being experimentally known, if $\Gamma_1{}^p$ or $\Gamma_1{}^n$ is measured, we have enough equations to determine Δu, Δd, Δs and the sum ΔΣ= Δu+Δd+Δs which represents the total contribution of the quarks to the spin of the nucleon. Notice that the QCD corrections have a large effect (see Sect. 3).

Let us recall there that, for the EMC-SLAC experiments quoted in the introduction, it was claimed that experimental results lead to $\Gamma_1{}^p$=0.126±0.018, then to ΔΣ=0.12±0.18 (almost no contribution of the quarks to the nucleon spin!) and Δs=-0.19±0.06 (rather large contribution of the strange quark to the nucleon spin!).

2 – The SLAC experiments :

The E142 experiment has been made in Fall 1992. It is a measurement of the deep inelastic scattering of a polarized electron beam by a polarized ^{3}He target. The results of this experiment have been published[6]. The E143 experiment has been made from Oct. 93 until Feb. 94. It is also a DIS reaction but on polarized NH_3 and ND_3 targets. The results of this experiment are still under analysis and the results presented here are preliminary.

For both E142 and E143 experiments, the measured observables are the asymmetries:

$$A_{\|} = \frac{\sigma(\downarrow\uparrow) - \sigma(\uparrow\uparrow)}{\sigma(\downarrow\uparrow) + \sigma(\uparrow\uparrow)} \quad \text{and} \quad A_{\perp} = \frac{\sigma(\downarrow\leftarrow) - \sigma(\uparrow\leftarrow)}{\sigma(\downarrow\leftarrow) + \sigma(\uparrow\leftarrow)}$$

They are related to the spin structure functions $g_1(x)$ and $g_2(x)$ by the equations:

$$A_{\|} = \frac{g_1(x) - kg_2(x)}{2K\sigma} \quad \text{and} \quad A_{\perp} = \frac{g_1(x) + k'g_2(x)}{2K'\sigma}$$

where k, K, k', K' are kinematical factors.

In the kinematical conditions of the experiment, k is small, and, at first order:

$$g_1(x) \simeq \frac{A_{\|} \times F_2(x)}{2xD(1+R)}$$

where $F_2(x)$ is the spin averaged nucleon structure function, D and R are quantities related to the photo-absorption cross-sections of the virtual photon. In fact, in the experiments, we measured accurately $A_{//}$ but also (less precisely in E142) $A_{\perp}$ to derive g_1 without the above approximation. In E143, the accuracy on $A_{//}$ and $A_{\perp}$ is good enough to extract g_2 with a significant accuracy. Note that $A_{//}$ and $A_{\perp}$ are related to the virtual photon-nucleon longitudinal and transverse asymmetries, A_1 and A_2, respectively, by the equations:

$$A_{\|} = D(A_1 + \eta A_2) \quad \text{and} \quad A_{\perp} = d(A_1 - \eta A_2)$$

The main characteristics of these SLAC experiments are what follows:

– They lead to an "almost direct" measurement of $g_1^p(x)$ and $g_1^n(x)$ since, within small and well controlled nuclear corrections, the ^3He, NH_3 and ND_3 polarized targets used are, as for the spin is concerned, equivalent to polarized neutron, proton and proton+neutron targets, respectively.

– They are high luminosity and high polarizations experiments, which leads to low statistical errors.

– The beam polarization is reversed randomly 120 times per second, which allows to reduce considerably the systematic errors in these asymmetries measurements. The reversal, from time to time, of the target polarization also contributes to this reduction of systematic errors since it permits to eliminate some possible false asymmetries.

The experimental apparatus used in these experiments is almost the same. It has been described[6,7]. Let us recall here the main aspects of the E143 experiment:

– The electron beam is delivered by the Stanford Linear Accelerator Center, at Stanford, California, USA. It is a pulsed beam (120 spills of $\sim 2\ \mu s$ width every second). To avoid a heating of the cryogenic frozen target resulting in a loss of polarization, we were obliged to limit the beam intensity to 2 to 4×10^9 e^- per spill. We used beam energies of 9.7, 16.2 and 29.1 GeV. Before being accelerated, the electrons came from a polarized source where they were produced by illumination of a new strained-lattice GaAs photocathode by a circularly polarized flash-lamp-pumped Ti-sapphire laser operating at 850 nm[8]. The e^- polarization P_b obtained in these new conditions was very high and stable during the runs: it varied weakly from 0.83 to 0.86 in accordance with the monitored small variations of the quantum efficiency of the photocathode. It was measured by Möller scattering in 1-arm and 2-arm polarimeters close to the target, with an accuracy of $\sim$2%. The change of sign of the laser polarization allowed to change the polarization sign of the electron beam.

– The polarized NH_3 and ND_3 targets are made of granules of very pure p- or d-ammonia frozen in liquid He maintained at 1°K by a high-power evaporation refrigerator. To avoid to heat the target, the beam was rastered over the 4.9 cm^2 front surface of the target on a pulse to pulse basis. A superconducting Helmholtz coil provided a uniform field of 4.8 T. The ammonia, pre-irradiated before the experiment to create a dilute population of paramagnetic atoms, was exposed to 138 GHz microwaves to align the nucleon spins by hyperfine transition. For NH_3, the polarization P_t reached values up to 80% in 10 to 20 minutes then, under beam, decreased down to 50–55% in $\sim$10 hours, due to radiation damages. This was periodically repaired by annealing the target at 80°K. For the ND_3 target, the corresponding values of the polarization were around twice less. The target polarization was measured using NMR technique and the relative error is estimated to be $\sim$2.5%. The dilution factor f of polarized nucleons in the target varied with x_{Bj} from 0.13 to 0.17 for NH_3 and from 0.22 to 0.25 for ND_3.

Data were taken for the 4 combinations of the target and beam polarization directions. The measured asymmetries were quite consistent within the estimated errors bars.

– The scattered electrons were detected in 2 independent spectrometers shown in figure 1, located at 4.5° and 7° and allowing detection of electrons at energies ranging from 6 to 25

GeV. This experimental arrangement allowed to cover a kinematical range of $0.029<x<0.8$ with $Q^2>1.3$ $(GeV/c)^2$. The total amount of good e^- collected on tape was 2×10^8.

Each spectrometer was equipped with 2 Cerenkov counters in coïncidence and with a 200 lead-glass blocks Shower Counter (SC), to identify electrons among the numerous pions reaching the detection (up to 10 times more pions than e^- in the kinematical region of low x_{Bj}). The use of a neural network approach in analyzing the SC data greatly improved the π-e^- separation. Three hodoscopes were used to make tracking for systematic studies and for energy calibration of the shower counter. Measurements of energy and position in the shower counter as well as using tracking gave x and Q^2 for each electron identified. The two spectrometers were designed in such a way that real photons produced in the target could reach the detection only in making 2 bounces on the walls inside the spectrometers. This feature reduced a lot the single rate in the detectors, especially for the hodoscopes which were made of plastic scintillators.

– The experimental asymmetries $A_{//}$ and $A_{\perp}$ were determined using the equation:

$$A_{\parallel}\,(\text{or } A_{\perp}) = \left(\frac{N_- - N_+}{N_- + N_+}\right)\frac{C_N}{fP_bP_t} + A_{RC}$$

where N_+ or N_- stand for the number of scattered electrons for positive and negative beam polarization, C_N is a correction factor for the polarization of nitrogen, f, P_t and P_b are the dilution factor and the polarization of the target, and the polarization of the beam, respectively. A_{RC} is the radiative correction, evaluated according to Kukhto and Shumeiko[9] ("internal" corrections) and Tsai[10] ("external" corrections).

Then, to derive $g_1(x)$ with the formulae given above, we used the values obtained from the SLAC global fit[11] for R and the NMC global fit[12] for F_2. Using the SLAC global fit for the latter leads to similar results.

3 – Results and analysis :

The results obtained from the measurements in the E143 experiment for the ratio g_1/F_1 and for g_1 are presented in fig.1 and fig.2 for the proton. For the deuteron, preliminary results for g_1/F_1 and g_1 are presented in fig. 3 and fig. 4. Since no significant Q^2 dependence was observed at given x, the data at different energies have been averaged over Q^2 for each x bin.

Over the kinematical range covered, the integrals of g_1 obtained are

$$\int_{0.029}^{0.8} g_1^p(x)dx = 0.120 \pm 0.004 \text{ (stat)} \pm 0.009 \text{ (syst)}$$

and

$$\int_{0.029}^{0.8} g_1^d(x)dx = 0.042 \pm 0.004 \text{ (stat)} \pm 0.003 \text{ (syst)}$$

Extrapolating up to x=1 assuming a $(1-x)^3$ behavior for g_1 at large x leads to contributions of 0.001±0.001 for proton and 0.000±0.001 for deuteron. The extrapolation at low x down to 0 is more model dependant. Taking g_1 as a constant at low x, which is suggested by the data and compatible with Regge theory, we obtain contributions to the g_1-integral of 0.008±0.001±0.005 for the proton and 0.002±0.001 for the deuteron. So, finally:

$$\Gamma_1^p = \int_0^1 g_1^p(x)dx = 0.129 \pm 0.004 \text{ (stat)} \pm 0.010 \text{ (syst)}$$

and

$$\Gamma_1^d = \int_0^1 g_1^d(x)dx = 0.044 \pm 0.004 \text{ (stat)} \pm 0.004 \text{ (syst)}$$

Using the relation

$$\Gamma_1^p + \Gamma_1^n = \frac{2\Gamma_1^d}{(1 - 1.5\omega_D)}$$

where ω_D is the D-state probability in the deuteron, we obtain

$$\Gamma_1^n = \int_0^1 g_1^n(x)dx = -0.033 \pm 0.008 \text{ (stat)} \pm 0.013 \text{ (syst)}$$

Within the errors bars, these results are compatible with recent measurements on the neutron[6] (E142), the proton[13] and the deuteron[14] (SMC).

As for the Ellis-Jaffe sumrule, while our result for $\Gamma_1{}^n$ is compatible with the −0.010±0.005 predicted value, our experimental result for $\Gamma_1{}^p$ is clearly well-below the 0.160±0.007 value predicted by theory. Predicted values quoted here are QCD-corrected[15] up to the 3-order of the leading constant α_s.

As for the Björken Sum Rule, we obtain from our E143 measurements:

$$\Gamma_1^p - \Gamma_1^n = \int_0^1 \left(g_1^p(x) - g_1^n(x)\right) dx = 0.162 \pm 0.024$$

The prediction of Björken updated with the QCD corrections is $\Gamma_1^p - \Gamma_1^n = 0.171 \pm 0.008$. So, within the error bars and provided that QCD corrections are taken into account, there is no violation of the Björken sumrule.

Then, as explained in Sect. 1, we have extracted from our data the quantities Δu, Δd, Δs and their sum $\Delta\Sigma$= Δu+Δd+Δs, applying the perturbative corrections[15] according to the formulation given in Sect. 1 and using, for each experiment, the α_s value corresponding to the average Q^2 of the experiment (α_s=0.39 for Q^2=2 and α_s=0.35 for Q^2=3). In these calculations, we have used: F+D=1.2573±0.0028 and F/D=0.575±0.016[16]. The result for $\Delta\Sigma$ is presented in fig. 5, as a function of this averaged Q^2. One can see that, with the full QCD corrections, all the experiments are compatible with the average value $\Delta\Sigma$=0.32±0.04, well determined now with the precise E143 measurements. It must also be noted that the values extracted without QCD corrections (black stars in fig. 5, with errors bars of the same order than for the fully corrected points) are not consistent all together, since for proton and deuteron, the QCD corrections are large and opposite. It appears very clearly from fig. 5 that, due to this last property, the $\Delta\Sigma$ extracted from deuteron experiments are much more insensitive to QCD corrections than in the case of proton or neutron. At last, it is very interesting to notice that the average $\Delta\Sigma$ value extracted from experiments agrees extremely well with a two-phase chiral invariant quark bag model prediction made before the experiments, and which predicts also reasonable F and D values and satisfies the Björken sumrule[17].

Conclusions and future plans

Our E143 experiment has provided measurement of the spin structure functions g_1 and g_2 of the proton and of the deuteron. The determination of g_2 is still under analysis. As for g_1, these measurements are in good agreement with the previous data, but have smaller errors, specially for the deuteron. The fundamental Björken sumrule on the first moments is satisfied, provided that QCD corrections are properly taken into account. In the frame of the Quark Parton Model with QCD corrections up to the 3–rd order in α_s, the total contribution of the quarks to the spin of the nucleon is then (32±4)%, and the non-zero contribution of the s-strange quark is (−9±2)%. In the kinematical domain of the experiment, we do not see Q^2 dependence at given x_{Bj} of g_1/F_1 or of A_1 within the error bars.

An increase of the beam energy to 50 GeV is scheduled for 1995. It will allow to reach smaller x values and other Q^2 values at given x. The same measurements of $A_{//}$ and $A_\perp$ will be repeated at this energy. All data together will allow to test the Q^2 in a large range, i.e. will allow to check the theoretical estimates of the QCD corrections quoted in the previous paragraph.

References :

1 – M. J. Alguard et al, Phys. Rev. Lett. 37(1976)1258; 37(1976)1261;41(1978)70.

2 – G. Baum et al, Phys. Rev. Lett. 51(1983)1135.

3 – J. Ashman et al, Phys. Lett. B206(1988)364; Nucl. Phys. B328(1989)1.

4 – J. Ellis and R. Jaffe, Phys. Rev. D9(1974)1444;D10(1974)1669.

5 – J. D. Björken, Phys. Rev. 148(1966)1467; Phys. Rev. D1(1970)1376.

6 – P. L. Anthony at al (E142), Phys. Rev. Lett. 71(1993)959.

7 – K. Abe et al (E143), Submitted to Phys. Rev. Lett.

8 – T. Maruyama et al, Phys. Rev. B46(1992)4261;
R. Alley et al, Report No. SLAC-PUB-6489 (1994).

9 – T. V. Kukhto and N. M. Shumeiko, Nucl. Phys. B219(1983)412;
I. V. Akusevich and N. M. Shumeiko, J. Phys. G20(1994)513.

10 – Y. S. Tsai, Report SLAC-Pub-848, 1971;
Y. S. Tsai, Rev. of Mod. Phys. 46(1974)815.

11 – L. W. Whitlow et al, Phys. Lett. B250(1990)193; B282(1992)475.

12 – P. Amaudruz et al (NMC), Phys. Lett. B295(1992)159.

13 – B. Adeva et al (SMC), Phys. Lett. B302(1993)533.

14 – D. Adams at al (SMC), Phys. Lett. B329(1994)399.

15 – S. A. Larin et al, Phys. Rev. Lett. 66(1991)862;
Phys. Lett. B259(1991)345; Phys. Lett. B334(1994)192.

16 – F. E. Close and R. G. Roberts, Phys. Lett. B316(1993),165.

17 – H. Høgaasen and F. Myhrer, Phys. Lett. B214(1988)123; Z. Phys. C48(1990)295.

Figures captions :

1 – Experimental results for the ratio g_1/F_1 versus x_{Bj} for the proton. Errors bars are statistical. Systematic uncertainties are shown at the bottom of the figure. Comparison with previous data is also presented.

2 – Experimental results for the structure function g_1 versus x_{Bj} for the proton. Errors bars are statistical.

3 – Experimental results for the ratio g_1/F_1 versus x_{Bj} for the deuteron (preliminary data). Errors bars are statistical. Comparison with previous data from SMC is also presented.

4 – Experimental results for the structure function g_1 versus x_{Bj} for the deuteron (preliminary data). Errors bars are statistical.

5 – Total quark contribution to the nucleon spin derived in the Quark Parton Model for all experiments, versus the average Q^2 of each experiment. For each experiment, the result is plotted without QCD correction (black star), with second order corrections (open star) and with the full corrections[15] (open circle) calculated with α_s values corresponding to the average Q^2 of the experiment.

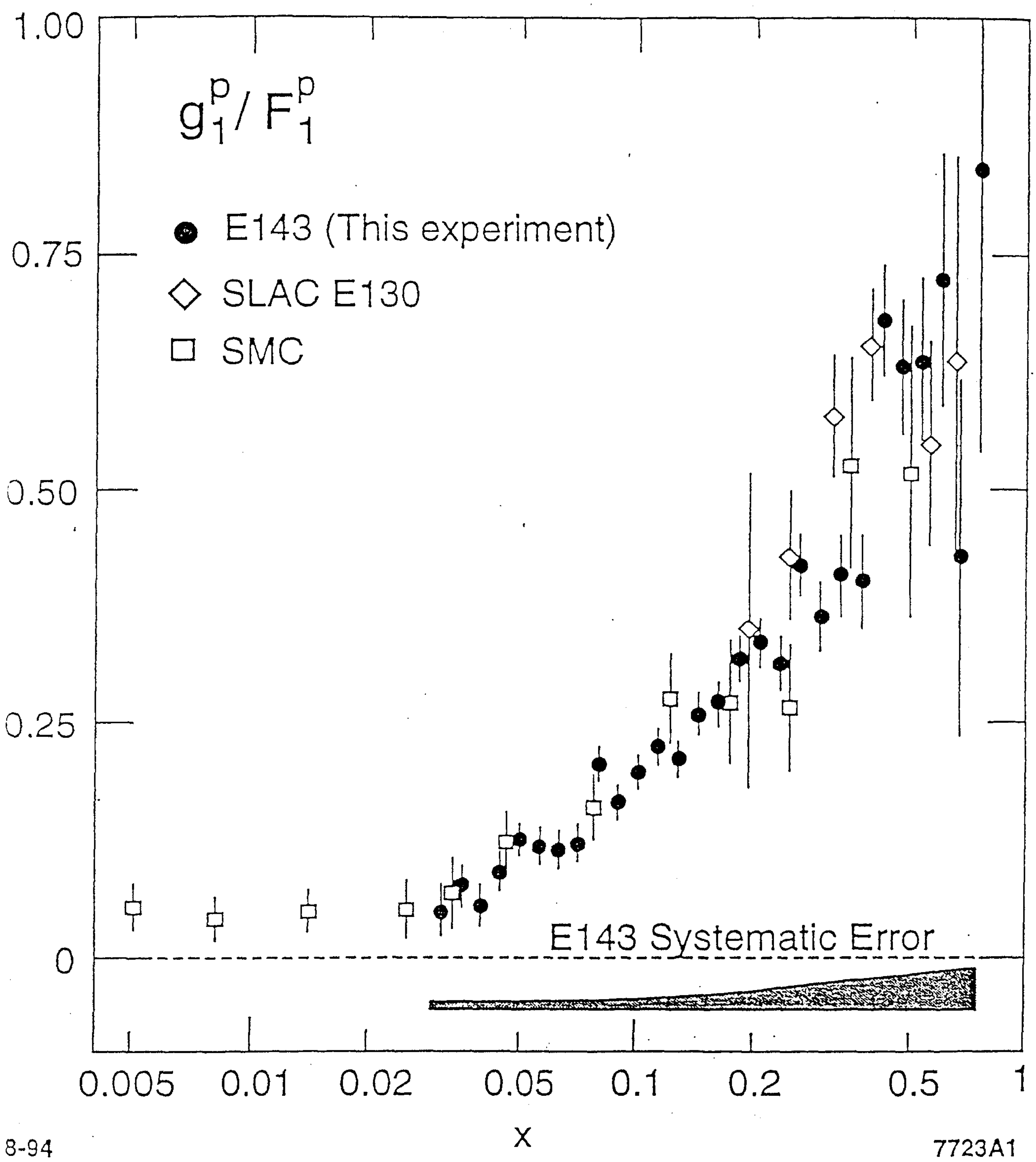

1.00
0.75
0.50
0.25
0
g_1^p / F_1^p
E143 (This experiment)
SLAC E130
SMC
E143 Systematic Error
0.005
0.01
0.02
0.05
0.1
0.2
0.5
1
x
8-94
7723A1

Fig. 1

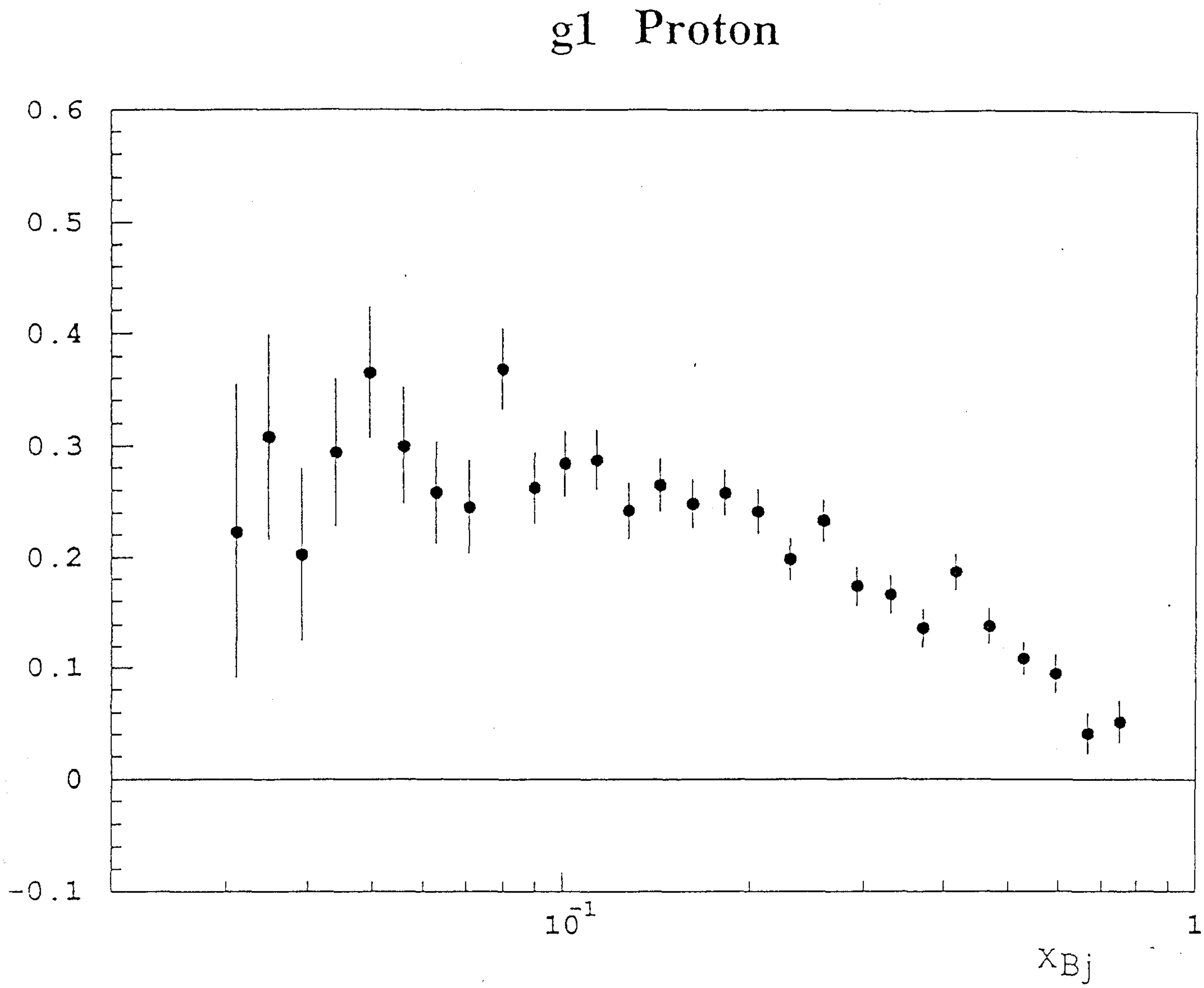

Fig. 2

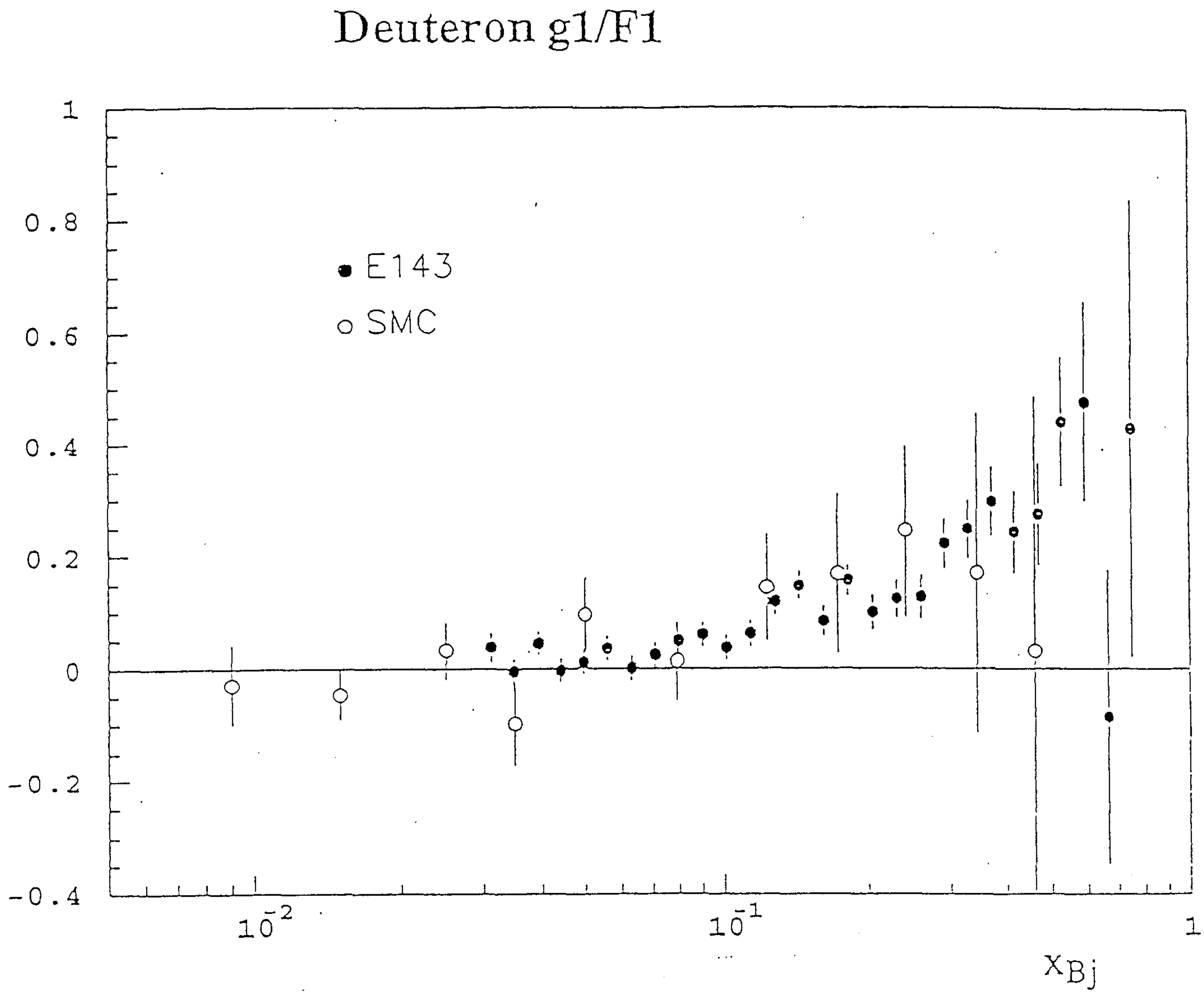

Fig. 3

Deuteron g1

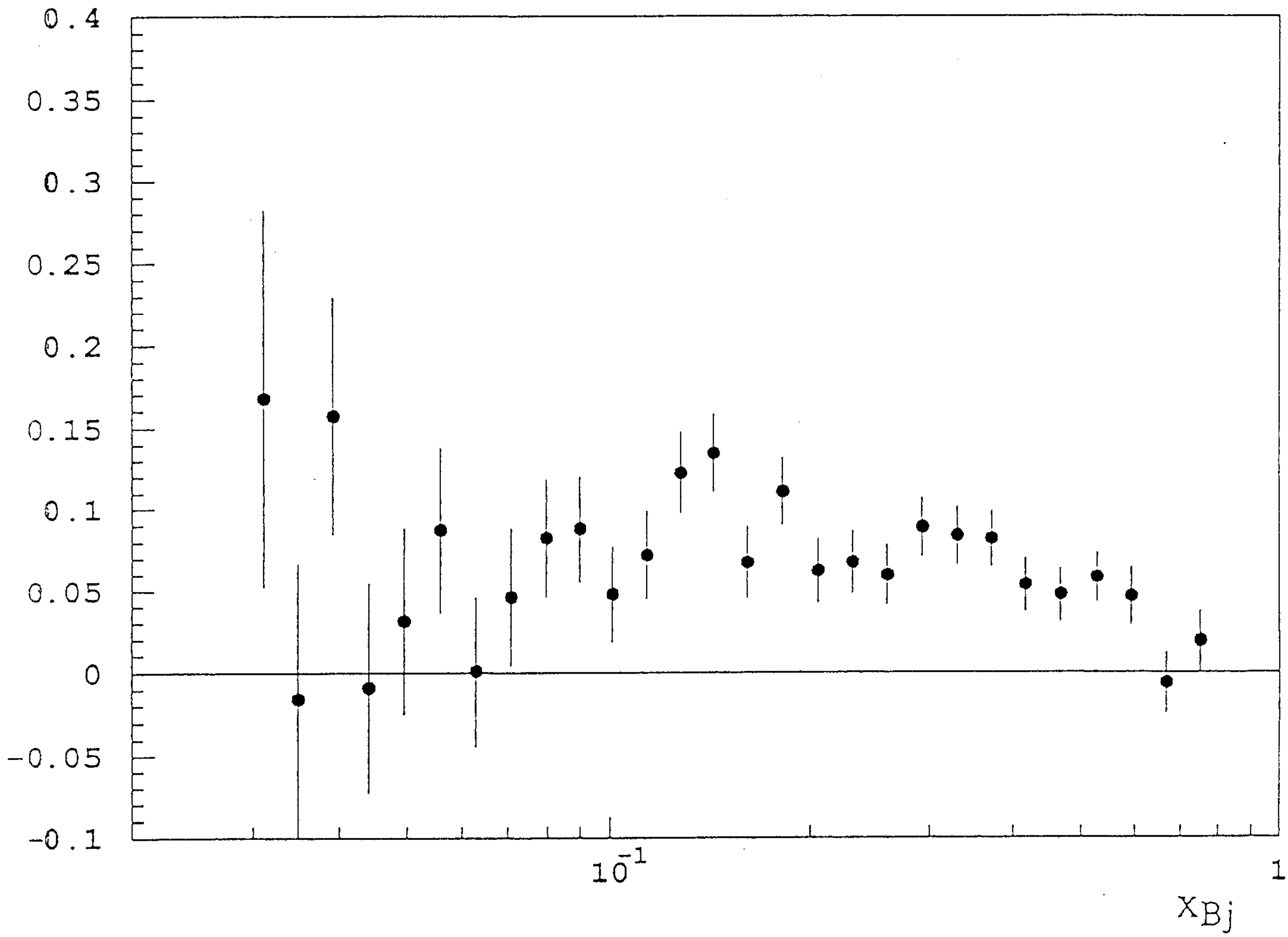

Fig. 4

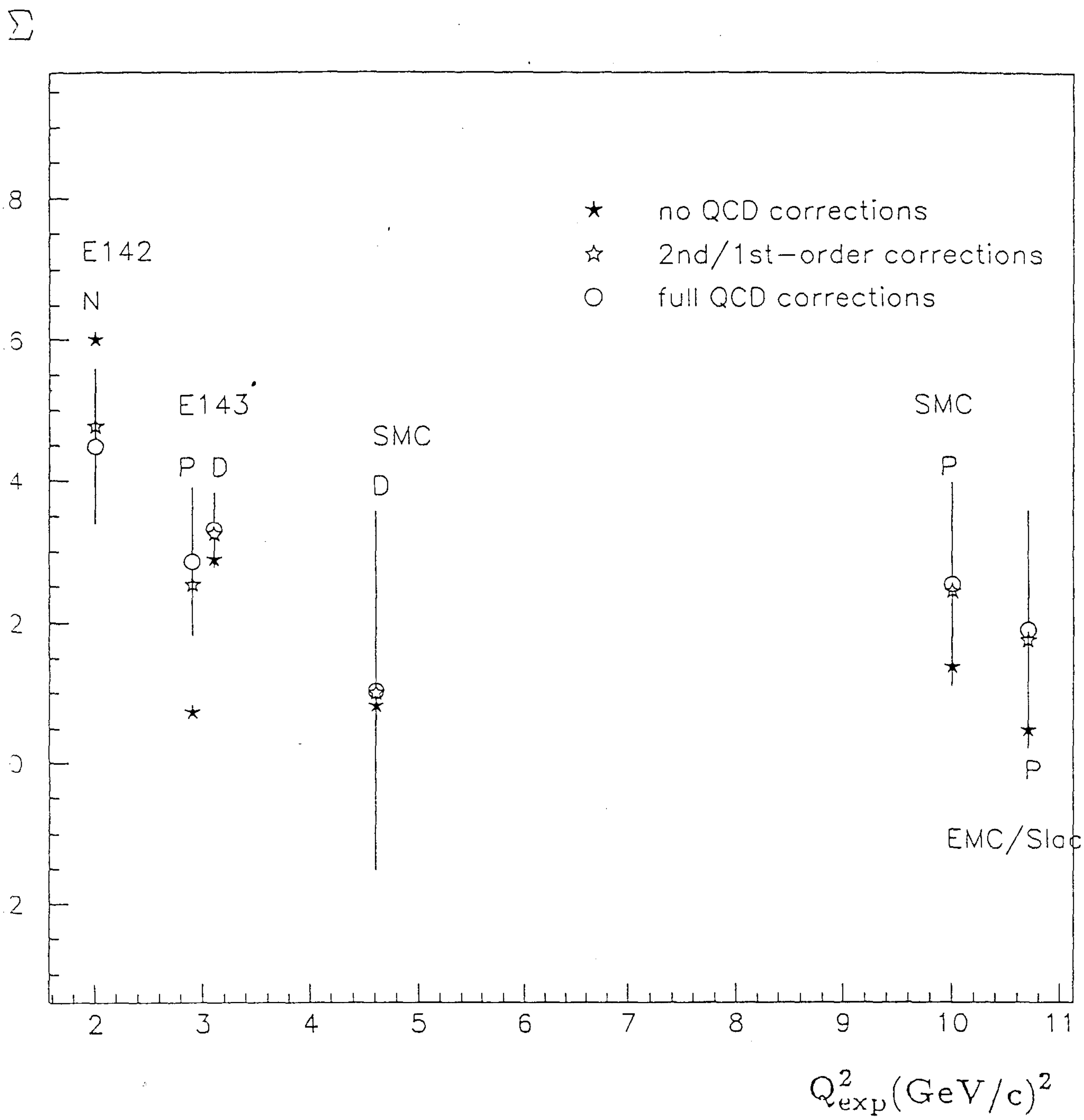

Σ
.8
.6
.4
.2
0
-.2
2
3
4
5
6
7
8
9
10
11
$Q^2_{exp} (GeV/c)^2$
no QCD corrections
2nd/1st−order corrections
full QCD corrections
E142
N
E143
P D
SMC
D
SMC
P
P
EMC/Slac

Fig. 5